Physics Letters B 709 (2012) 390–395

Contents lists available at SciVerse ScienceDirect

Physics Letters B

www.elsevier.com/locate/physletb

Microscopic spectral density of the Wilson Dirac operator for one flavor

Rasmus Normann Larsen

Niels Bohr International Academy and Discovery Center, Niels Bohr Institute, University of Copenhagen, Blegdamsvej 17, DK-2100 Copenhagen, Denmark

ARTICLE INFO

Article history:
Received 9 November 2011
Received in revised form 10 February 2012
Accepted 10 February 2012
Available online 17 February 2012
Editor: A. Ringwald

Keywords:
Wilson fermions
Microscopic limit

ABSTRACT

We consider the effect of a non-zero lattice spacing on the low-energy effective theory of Wilson fermions with $N_f = 1$. Analytical results are given for both the chiral condensate and the microscopic spectral density of the Wilson Dirac operator. It is observed that the partition function for a sector of fixed index ν has ν real zeros. A subtle mechanism ensures that a constant chiral condensate is recovered, once the sum over sectors ν is performed.

1. Introduction

The low energy effective theory of QCD is based on Goldstone bosons of the broken chiral symmetry $SU(N_f)_L \otimes SU(N_f)_R$. As is well known, the $U(1)$ axial symmetry is explicitly broken at the quantum level, because of the anomaly. This means that the $N_f = 1$ theory might appear quite trivial at low energy because there are no Goldstone bosons. Leutwyler and Smilga showed in [1] that this is not the case: an expansion of the partition function in terms of $me^{i\theta}$ for $N_f = 1$, shows that interesting behavior arises in sectors of fixed topology ν.

For simulations of QCD on the lattice, one faces the problem of doubling. For one flavor, the 15 extra states can be removed, by adding a Wilson term to the Dirac operator. We denote the Dirac operator with the Wilson term included by D_W. The addition of the Wilson term, moves the eigenvalues of the extra states away from the origin in bunches of 4, 6, 4, and 1. In continuum language the Wilson term is equivalent to a double derivative proportional to the lattice spacing a.

The Wilson term destroys the anti-hermiticity of the Dirac operator, only retaining γ_5-hermiticity, $D_W^\dagger = \gamma_5 D_W \gamma_5$. The hermitian operator $D_5 = \gamma_5(D_W + m)$ can still be defined. The eigenvalues for D_W spread in the complex plane, removing the apparent definition of a sector ν in terms of zero modes.

We explore the low energy behavior of the Wilson Dirac operator by using the low-energy effective field theory, for which we restrict ourself to the ϵ regime. For the $N_f = 1$ case, there is no spontaneous breaking of symmetry, but it is still possible to find a behavior very closely reminiscent of the ϵ-regime in chiral perturbation theory, if we focus on sectors of fixed index ν. A choice of definition of such sectors as the Fourier modes of the partition function, ensures a simple definition of ν, as the sum of the sign of chirality of the real modes [2].

We will explore the special case of $N_f = 1$. We start in Section 2 by recalling the low-energy effective theory for the Dirac operator for $N_f = 1$. In Section 3 we include the terms emerging from the Wilson term. In Section 4 we show how to obtain the chiral condensate, which will be used to find both the full condensate and the condensate for each sector of fixed index. We use this to see the number of real zeros when the lattice spacing is non-zero. We will in particular focus on how the full condensate is built up from sectors of fixed ν. In Section 5, we look at the spectral density of the hermitian Wilson Dirac operator D_5, as well as the corresponding ρ_χ, where we include two terms not previously considered in the $N_f = 1$ case.

2. N_f in the continuum

Here we recall the arguments of Leutwyler and Smilga [1] for $N_f = 1$. It was shown, that though there are no Goldstone bosons for $N_f = 1$, the effective partition function in the ϵ regime, where one confines to a box of size $L = \frac{1}{\epsilon}$ and $m \sim \epsilon^4$ [3], could be described by the exponential of minus the energy

$$Z(m,\theta) = e^{\Sigma V m \operatorname{Re}(e^{i\theta})}. \tag{1}$$

By use of the $U(1)$ axial anomaly, it was shown that the only parameter the energy would depend on was $me^{i\theta}$, for which the given result is the lowest order in m. The decomposition of a sector of fixed index in QCD

$$Z^\nu(m) = \langle m^{|\nu|} \Pi_k (\lambda_k^2 + mm^*) \rangle, \tag{2}$$

E-mail address: atoya@fys.ku.dk.

0370-2693
doi:10.1016/j.physletb.2012.02.038

was used to find the transformation properties. λ_k are the eigenvalues of the Dirac operator. These transformation properties could be mimicked in the effective partition function if the Fourier modes of Z, were chosen as the effective partition function for fixed index ν, i.e. Z^ν such that

$$Z(m,\theta) = \sum_\nu e^{i\theta\nu} Z^\nu(m). \tag{3}$$

3. Inclusion of lattice spacing

We now extend the argument of the previous section to non-zero a. The ϵ counting scheme for $a \neq 0$, is taken to be

$$m \sim a^2 \sim \epsilon^4 = V^{-1}, \tag{4}$$

such that first order terms in m are compatible with second order of a. The terms proportional to the lattice constant a are included in the effective theory, by the same principle as how the mass is included, as they both come from terms depending on $\bar\psi\psi$ [4]

$$\begin{aligned} VL_a = {} & Vc_0 \operatorname{Tr}\big(a\big(U+U^\dagger\big)\big) + VW_6\big(\operatorname{Tr}\big(a\big(U+U^\dagger\big)\big)\big)^2 \\ & + VW_7\big(\operatorname{Tr}\big(a\big(U-U^\dagger\big)\big)\big)^2 \\ & + VW_8 \operatorname{Tr}\big(aUaU + aU^\dagger aU^\dagger\big). \end{aligned} \tag{5}$$

The first term is of the same form as the first order term in m. We redefine both terms to $\frac{1}{2}\operatorname{Tr}(M(U+U^\dagger))$, where $V\Sigma m + VW_8 a \equiv M$. The remaining terms are set to $a^2W_6V \equiv a_6^2$, $a^2W_7V \equiv a_7^2$ and $a^2W_8V \equiv a_8^2$, which are all ~ 1 in the ϵ regime. For a general N_f with Goldstone bosons, this gives [5]

$$\begin{aligned} Z = {} & \int_{SU(N_f)} dU e^{\frac{1}{2}\operatorname{Tr}(M(U+U^\dagger))} \\ & \times e^{-a_6^2(\operatorname{Tr}(U+U^\dagger))^2 - a_7^2(\operatorname{Tr}(U-U^\dagger))^2 - a_8^2\operatorname{Tr}(U^2+(U^\dagger)^2)}. \end{aligned} \tag{6}$$

For $N_f = 1$ with no Goldstone bosons, we obtain the same form by adding terms with $ae^{i\theta}$, to the partition function, such that we only obtain real terms. We have chosen to add the phase to the lattice spacing a. In the ϵ regime this gives

$$Z(\theta,m,a) = \exp\big(m\cos(\theta) - 2a_8^2\cos(2\theta)\big). \tag{7}$$

The parts proportional to a_6^2 and a_7^2 have been omitted, because for $N_f = 1$ for the partition function, a_6^2, a_7^2 and a_8^2 can be redefined into a a_8^2 term. If the mode number of the Fourier modes of Z is chosen as a definition of the index ν for the lattice Dirac operator, then according to [2] the index ν is given by

$$\nu = \sum_k \operatorname{sign}\big(\langle k|\gamma_5|k\rangle\big), \tag{8}$$

which is only affected by the real eigenvalues λ, since λ with $\operatorname{Im}[\lambda] \neq 0$ then $\langle k|\gamma_5|k\rangle = 0$. With the inclusion of the $U(1)$ integral, Z^ν for $N_f = 1$ is defined by [8]

$$Z^\nu(m,a_8) = \int_{-\pi}^{\pi} d\theta \exp\big(i\nu\theta + m\cos(\theta) - 2a_8^2\cos(2\theta)\big). \tag{9}$$

4. The chiral condensate for $N_f = 1$

We are interested in the analytic behavior for one flavor $N_f = 1$ with $a \neq 0$. The chiral condensate is found from the partition function

$$\Sigma\big(m,a_8^2,\theta\big) = \frac{\partial}{\partial m}\log\big(Z\big(\theta,m,a_8^2\big)\big). \tag{10}$$

For one flavor using (7) we obtain

$$\Sigma\big(m,a_8^2,\theta\big) = \cos(\theta), \tag{11}$$

which is exactly as found in [6] in the continuum. This result is in contrast to the much more complicated condensate for each sector ν, $\Sigma^\nu(m,a_8)$, which is given by

$$\Sigma^\nu\big(m,a_8^2\big) = \frac{\int_{-\pi}^{\pi} d\theta\cos(\theta)\exp(i\nu\theta + m\cos(\theta) - 2a_8^2\cos(2\theta))}{\int_{-\pi}^{\pi} d\theta\exp(i\nu\theta + m\cos(\theta) - 2a_8^2\cos(2\theta))}. \tag{12}$$

Making the change $\theta \to -\theta$ in both integrals, it is seen that $\Sigma^\nu = \Sigma^{-\nu}$. It is also observed that

$$\begin{aligned} Z^\nu(m,a_8) &= \int_0^{2\pi} e^{i\nu\theta} e^{m\cos(\theta) - 2a_8^2\cos(2\theta)}\, d\theta \\ &= \int_{-\pi}^{\pi} e^{i\pi\nu} e^{i\nu\theta} e^{-m\cos(\theta) - 2a_8^2\cos(2\theta)}\, d\theta \\ &= Z^\nu(-m,a_8)(-1)^\nu. \end{aligned} \tag{13}$$

For $a_8^2 = 0$, $Z^\nu(m,a_8^2)$ has a zero of ν'th order in 0. For $a_8^2 \neq 0$ it is observed that these zeros spread out into pairs as just predicted from Eq. (13). Expanding to first order in a_8^2 and ν'th order in m, one finds the behavior to be

$$\begin{aligned} Z^{\nu=2} &\approx m^2/8 - a_8^2 - a_8^2m^2/4, \\ Z^{\nu=3} &\approx m^3/48 - a_8^2m/2 - a_8^2m^3/16, \end{aligned} \tag{14}$$

where the zeros are found to be linearly dependent on a_8. For larger a_8 the dependence becomes quadratic, see Fig. 1.

For larger m and a_8^2 than seen in Fig. 1, the zeros become harder to see in plots as those in Fig. 1. We have therefore plotted for fixed $a_8^2 = 10, 20, \ldots, 100, 200, \ldots, 1000, \ldots, 10\,000$, where one of these plots is shown in Fig. 2.

It was observed that in all plots, the number of zeros is equal to the index ν.

We are also interested in finding how each sector adds to the full chiral condensate

$$\begin{aligned} \Sigma(\theta) &= \frac{\partial}{\partial m}\log\left(\sum_{\nu=-\infty}^{\infty} e^{i\nu\theta} Z^\nu\right) \\ &= \frac{\sum_{\nu=-\infty}^{\infty} e^{i\nu\theta}\partial_m Z^\nu}{\sum_{\nu=-\infty}^{\infty} e^{i\nu\theta} Z^\nu} \\ &= \sum_{\nu=-\infty}^{\infty} e^{i\nu\theta}\Sigma^\nu Z^\nu/Z. \end{aligned} \tag{15}$$

This tells us that we should weight each sector ν with the factor $e^{i\nu\theta}Z^\nu/Z$, such that Z^ν cancels the poles. In Fig. 3 we show the convergence of the sum over ν for $\theta = 0$.

The higher terms cancel the too high values around $m = 0$, and this cancellation overshoots, such that Σ at $m = 0$ oscillates, though converging towards $\Sigma = 1$. We compare this to the $a_8^2 = 0$ case in Fig. 4.

We find that the sector $\nu = 0$, is not too significant, as there is no contribution to Σ at $m = 0$, and Σ^0 in no way fills up most of Σ. That Σ^0 is almost 1 at $m = 1$ in Fig. 3 is a coincidence and is not true for other a_8^2.

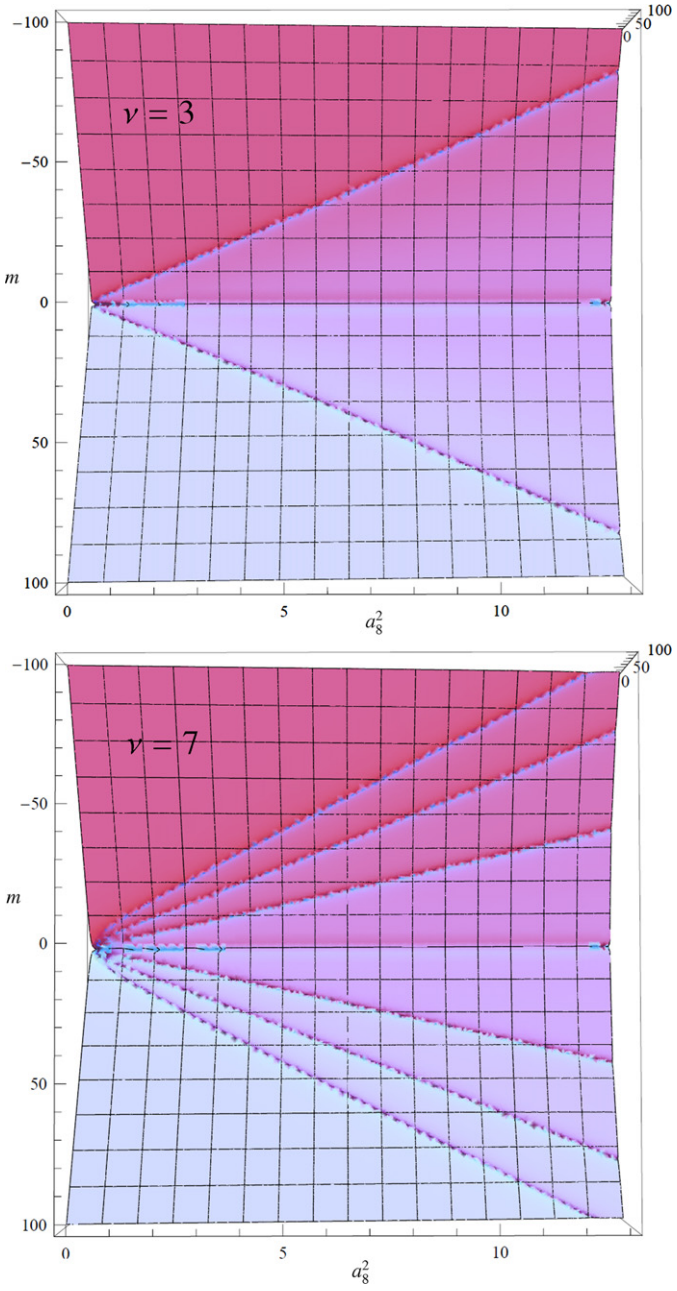

Fig. 1. Zeros for Z^ν. The plot shows a 3d plot for $\log(Z^\nu)$ seen from above for $\nu = 3$ and 7 respectively, where the x-axis is a_8^2 and the y-axis is m. The zeros of Z^ν are seen as the lines, since the logarithm blows up at $Z^\nu = 0$.

While we see how different the picture is, it is important to note that this is mainly if one focuses on the pole behavior around $m = 0$. As one passes the poles at around $m = 8a_8^2$, the behavior quickly goes to that of $a_8^2 = 0$. We show this in Fig. 5.

5. The density with a_6^2 and a_7^2

For $N_f = 1$, we redefined a_6^2 and a_7^2 into a_8^2, such that Z^ν was only dependent on a_8^2. For the spectral densities of the Wilson Dirac operator, this is not the case. As in [2], we expand the partition function to

$$Z_{(2|1)}(M, Z, a_i) = \left\langle \frac{\det(D_W + m_f + z_f\gamma_5)\det(D_W + m + z\gamma_5)}{\det(D_W + m' + z'\gamma_5)} \right\rangle,$$

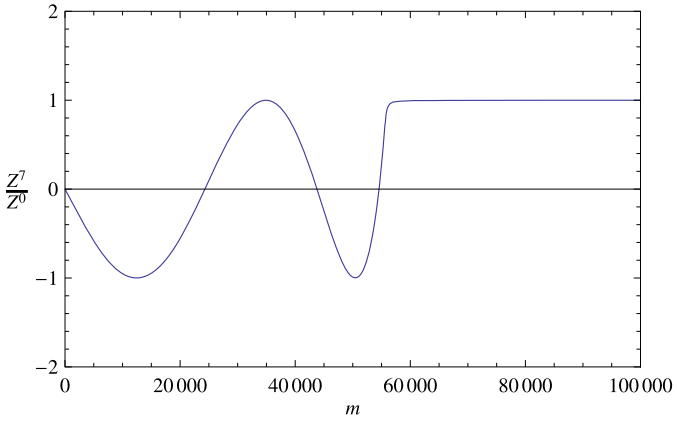

Fig. 2. Z^7/Z^0 for $a_8^2 = 7000$. Z^0 is used to normalize, since it is always positive.

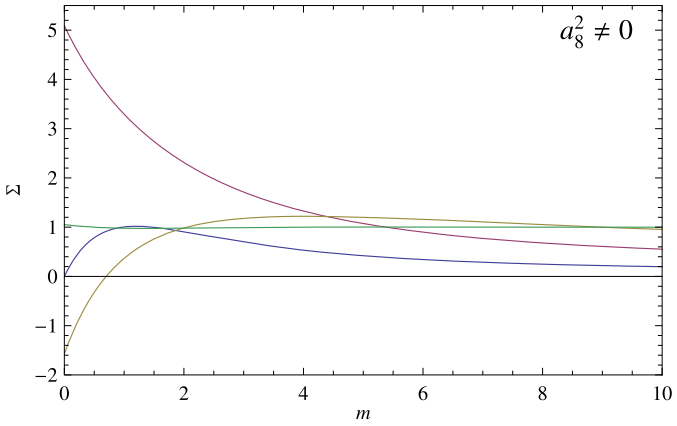

Fig. 3. The oscillating behavior $\sum_{\nu=-j}^{j} Z^\nu \Sigma^\nu / Z$ for $a_8^2 = 1.5$ and $j = 0, 1, 3, 9$. The curve for $j = 0$ is 0 at $m = 0$, $j = 1$ is the largest and $j = 9$ is almost 1.

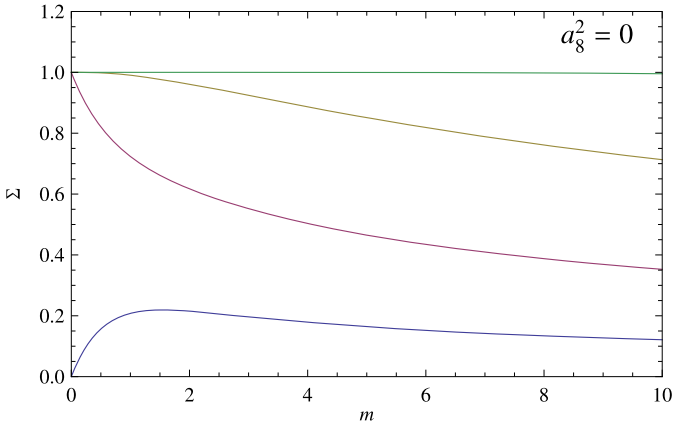

Fig. 4. $\sum_{\nu=-j}^{j} Z^\nu \Sigma^\nu / Z$ for $a_8^2 = 0$ and $j = 0, 1, 3, 9$. $j = 0$ is the smallest and the graphs builds up towards $\Sigma = 1$, which is almost true for $j = 9$.

where we have included the γ_5-mass term, which is proportional to Z. We have also defined $M = \mathrm{diag}(m_f, m, m')$ and $Z = \mathrm{diag}(z_f, z, z')$. We have added one extra bosonic flavor and one more fermionic flavor. The partially quenched condensate is then defined as

$$\Sigma^\nu(m_f, m) = \frac{\partial}{\partial m}\left(\log\left(Z^\nu_{(2|1)}(m_f, m, m')\right)\right)\Big|_{m=m'}, \tag{16}$$

where $z_f = z = z' = 0$ and a_6^2, a_7^2 and a_8^2 are included, but not shown. It was shown in [2] that spectral densities could be obtained by taking the discontinuity, which for $\Sigma^\nu(m_f, m)$ obey

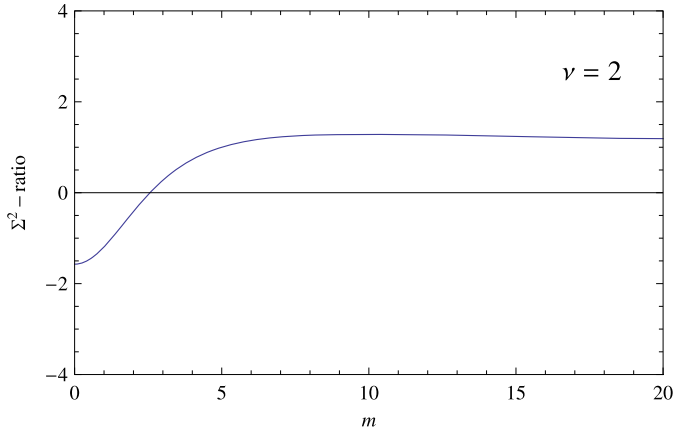

Fig. 5. $\Sigma^2(a_8^2 = 0)/\Sigma^2(a_8^2 = 1)$. The ratio for the chiral condensate between the continuum and the lattice effective theory for a fixed sector $\nu = 2$, is seen to converge to 1, when m is away from the area of the poles of $\Sigma^2(a_8^2 = 1)$.

$$\rho_\chi^\nu(\lambda^W, m_f) = \left\langle \sum_k \delta\big(\lambda_k^W + \lambda^W\big)\,\mathrm{sign}\big[\langle k|\gamma_5|k\rangle\big] \right\rangle_\nu = \frac{1}{\pi}\,\mathrm{Im}\big[\Sigma^\nu(m_f, m)\big]\big|_{m=\lambda^W}, \tag{17}$$

where $\mathrm{sign}[\langle k|\gamma_5|k\rangle]$ was included for regularization. λ_k^W are the eigenvalues of D_W. The extra quarks result in an enlarged symmetry group, and we therefore need to integrate over the largest convergent sub-group of $GL(2|1)$ as described in [7]. While the Grassmann integrations trivially converge, the bosonic integrals need careful attention. Following [2] we rotate $U \to iU$ to make Z^ν convergent for positive a_8^2, such that

$$Z_{(2|1)}^\nu = \int dU\,\mathrm{Sdet}(U)^\nu \exp\bigg(\frac{i}{2}\,\mathrm{Str}\big(M\big(U - U^{-1}\big)\big) + a_6^2\,\mathrm{Str}\big(U - U^{-1}\big)^2 + a_7^2\,\mathrm{Str}\big(U + U^{-1}\big)^2 + a_8^2\,\mathrm{Str}\big(U^2 + U^{-2}\big) + \frac{i}{2}\,\mathrm{Str}\big(Z\big(U + U^{-1}\big)\big)\bigg). \tag{18}$$

We choose the parametrization

$$U = \begin{pmatrix} e^{it+iu}\cos(\theta) & ie^{it+i\phi}\sin(\theta) & 0 \\ ie^{it-i\phi}\sin(\theta) & e^{it-iu}\cos(\theta) & 0 \\ 0 & 0 & e^s \end{pmatrix} \exp\begin{pmatrix} 0 & 0 & \alpha_1 \\ 0 & 0 & \alpha_2 \\ \beta_1 & \beta_2 & 0 \end{pmatrix},$$

for which the Berezinian becomes $J = 4\cos(\theta)\sin(\theta)(1 + \frac{1}{3}(\alpha_1\beta_1 + \alpha_2\beta_2))$ [7] and we define $|J_0| \equiv 4|\cos(\theta)\sin(\theta)|$. Plugging U into the partition function Z^ν, we find that the ϕ dependence disappears, and the ϕ integral simply gives π. The Grassmann integrals can also be carried out explicitly. This gives

$$Z_{(2|1)}^\nu\big(m_f, m, m', z_f, z, z', a_6, a_7, a_8\big) = \pi \int_{-\infty}^{\infty} ds \int_{-\pi}^{\pi} dt \int_{-\pi}^{\pi} du \int_{-\pi}^{\pi} d\theta\, e^{S_f + S_b + S_{67} + (2it - s)\nu} \times \bigg(P_4 - P_{11}P_{22} + P_{12}P_{21} - \frac{1}{3}(P_{11} + P_{22})\bigg)|J_0|, \tag{19}$$

which was done without a_6^2 and a_7^2 in [8]. The terms with a_6^2 and a_7^2 are a bit more complicated, but can still be reproduced here

$$\begin{aligned}
S_f &= \cos(\theta)\big(-m_f\sin(t+u) - m\sin(t-u) \\
&\quad + iz_f\cos(t+u) + 4a_8^2\cos(2t)\cos(2u)\cos(\theta) \\
&\quad + iz\cos(t-u)\big) - 4a_8^2\cos(2t)\sin^2(\theta), \\
S_b &= -im'\sinh(s) - iz'\cosh(s) - 2a_8^2\cosh(2s), \\
S_{67} &= 4a_6^2\big(2i\cos(\theta)\cos(u)\sin(t) - \sinh(s)\big)^2 \\
&\quad + 4a_7^2\big(2\cos(\theta)\cos(u)\cos(t) - \cosh(s)\big)^2, \\
P_{11} &= i\frac{1}{2}\big(\cos(\theta)\big(im_f\sin(t+u) + z_f\cos(t+u)\big) + m'\sinh(s) \\
&\quad + z'\cosh(s)\big) + a_8^2\big(2\cos(2t+2u)\cos^2(\theta) \\
&\quad - 2\cos(2t)\sin^2(\theta) \\
&\quad + 4\cosh(it+iu+s)\cos(\theta) + 2\cosh(2s)\big) \\
&\quad + 4a_6^2\big(2i\cos(\theta)\cos(u)\sin(t) - \sinh(s)\big) \\
&\quad \times \big(i\sin(t+u)\cos(\theta) + \sinh(s)\big) \\
&\quad + 4a_7^2\big(2\cos(\theta)\cos(u)\cos(t) - \cosh(s)\big) \\
&\quad \times \big(\cos(t+u)\cos(\theta) + \cosh(s)\big), \\
P_{22} &= i\frac{1}{2}\big(\cos(\theta)\big(im\sin(t-u) + z\cos(t-u)\big) + m'\sinh(s) \\
&\quad + z'\cosh(s)\big) + a_8^2\big(2\cos(2t-2u)\cos^2(\theta) \\
&\quad - 2\cos(2t)\sin^2(\theta) \\
&\quad + 4\cosh(it-iu+s)\cos(\theta) + 2\cosh(2s)\big) \\
&\quad + 4a_6^2\big(2i\cos(\theta)\cos(u)\sin(t) - \sinh(s)\big) \\
&\quad \times \big(i\sin(t-u)\cos(\theta) + \sinh(s)\big) \\
&\quad + 4a_7^2\big(2\cos(\theta)\cos(u)\cos(t) - \cosh(s)\big) \\
&\quad \times \big(\cos(t-u)\cos(\theta) + \cosh(s)\big), \\
P_{12} &= -\frac{1}{4}\sin(\theta)\big(m_f e^{-it} + me^{it} - z_f e^{-it} + ze^{it}\big) \\
&\quad - 4a_8^2\sin(\theta)\big(\sin(t-is) + \sin(2t)\cos(u)\cos(\theta)\big) \\
&\quad + 4a_6^2\big(2i\cos(\theta)\cos(u)\sin(t) - \sinh(s)\big)i\cos(t)\sin(\theta) \\
&\quad - 4a_7^2\big(2\cos(\theta)\cos(u)\cos(t) - \cosh(s)\big)\sin(t)\sin(\theta), \\
P_{21} &= -\frac{1}{4}\sin(\theta)\big(m_f e^{it} + me^{-it} + z_f e^{it} - ze^{-it}\big) \\
&\quad - 4a_8^2\sin(\theta)\big(\sin(t-is) + \sin(2t)\cos(u)\cos(\theta)\big) \\
&\quad + 4a_6^2\big(2i\cos(\theta)\cos(u)\sin(t) - \sinh(s)\big)i\cos(t)\sin(\theta) \\
&\quad - 4a_7^2\big(2\cos(\theta)\cos(u)\cos(t) - \cosh(s)\big)\sin(t)\sin(\theta), \\
P_4 &= \frac{i}{24}\cos(\theta)\big(im_f\sin(t+u) + im\sin(t-u) + z_f\cos(t+u) \\
&\quad + z\cos(t-u)\big) + \frac{1}{12}\big(m'\sinh(s) + z'\cosh(s)\big) \\
&\quad + a_8^2\bigg(\frac{1}{3}\cos(2t)\cos(2u)\cos^2(\theta) + \cos(2t)\cos^2(\theta) \\
&\quad + \frac{2}{3}\cos(2t)\sin^2(\theta) + \frac{8}{3}\cosh(it+s)\cos(u)\cos(\theta) \\
&\quad + \frac{4}{3}\cosh(2s)\bigg) + 2a_6^2\bigg(\frac{1}{3}\big(2i\cos(\theta)\cos(u)\sin(t) - \sinh(s)\big) \\
&\quad \times \big(i\cos(\theta)\cos(u)\sin(t) + \sinh(s)\big) \\
&\quad - \big(i\sin(t+u)\cos(\theta) + \sinh(s)\big)\big(i\sin(t-u)
\end{aligned}$$

$$\times \cos(\theta) + \sinh(s)\big) - \sin(\theta)^2 \cos(t)^2\Big)$$
$$+ 2a_7^2\Big(\frac{1}{3}\big(2i\cos(\theta)\cos(u)\cos(t) - \cosh(s)\big)$$
$$\times \big(\cos(\theta)\cos(u)\cos(t) + \cosh(s)\big)$$
$$- \big(\cos(t+u)\cos(\theta) + \cosh(s)\big)$$
$$\times \big(\cos(t-u)\cos(\theta) + \cosh(s)\big) + \sin(\theta)^2\sin(t)^2\Big), \qquad (20)$$

for which convergence requires $0 > a_6^2 + a_7^2 - a_8^2$. Another representation can be found in [9]. We numerically solve the rest of the integrals to obtain the densities. In Fig. 6 we show a couple of densities for $N_f = 1$.

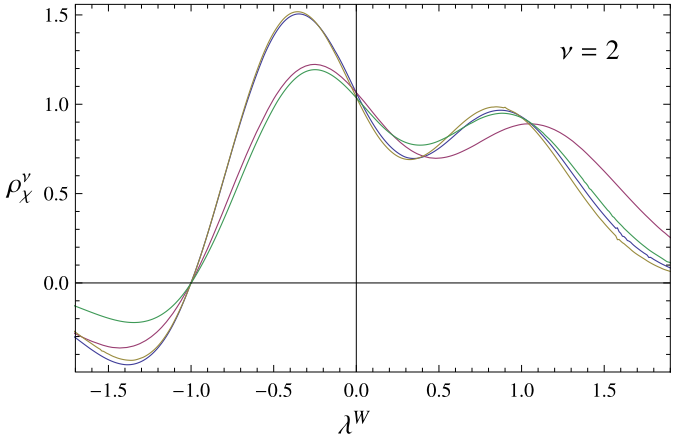

Fig. 6. The density ρ_χ^ν for sector $\nu = 2$ for $m_f = -1$ compared for different low-energy constants in the microscopic effective theory. At the right side the largest is $a_6^2 = 0.01, a_7^2 = 0, a_8^2 = 0.04$, the 2nd is $a_6^2 = 0, a_7^2 = 0, a_8^2 = 0.05$, the 3rd is $a_6^2 = 0, a_7^2 = 0.01, a_8^2 = 0.04$ and the smallest is $a_6^2 = a_7^2 = 0, a_8^2 = 0.04$.

It is seen how the addition of the a_6^2 and a_7^2 term changes the positions of the maxima and changes the values. It should be noticed how the density vanishes at $\lambda^W = -1$, as is required from the QCD partition function, since ρ_χ^ν is an average of $\sum_k \delta(\lambda^W + \lambda_k^W)\Pi_j(\lambda_j^W + m_f)$, which is always zero for $m_f = \lambda^W$.

The most important factor in how ρ_χ^ν looks, appears to be the ratio between m_f and the position of the peaks. This is seen from a series of graphs where we vary m_f. For m_f away from the maxima, the picture looks like that in Fig. 6, even though we use $a_8^2 = 0.2$ instead. Around the origin $Z^{\nu=2}$ changes sign, and we see a quite changed picture. We show this in Fig. 7.

When we defined the index ν for the partition function, we mentioned that the index ν is equal to the average of chirality for a configuration. For the density ρ_χ^ν this is equal to

$$\int_{-\infty}^{\infty} \rho_\chi^\nu(\lambda^W)\,d\lambda^W = \int_{-\infty}^{\infty}\left\langle \sum_k \delta(\lambda_k^W + \lambda^W)\,\mathrm{sign}\big[\langle k|\gamma_5|k\rangle\big]\right\rangle_\nu d\lambda^W$$
$$= \left\langle \sum_k \mathrm{sign}\big[\langle k|\gamma_5|k\rangle\big]\right\rangle_\nu = \nu. \qquad (21)$$

As a central self-consistency check, it has been verified by numerical integration, that this is true for the values of a_6^2, a_7^2 and a_8^2 in Figs. 6 and 7.

Finally we also consider the spectral density of the hermitian Wilson Dirac operator $D_5 = \gamma_5(D_W + m)$, obtained as in [2] by

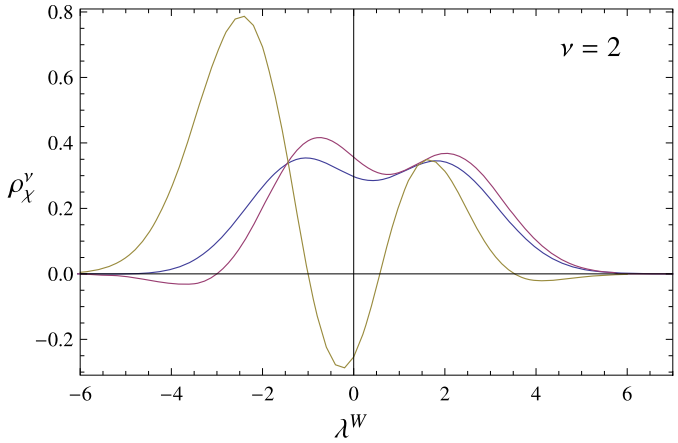

Fig. 7. $\rho_\chi^\nu(\lambda^W, m_f)$ for $\nu = 2$ and $a_8^2 = 0.2$ for $m_f = -5, -3, -1$. We see a completely different picture when the sign is flipped for $m_f = -1$. The graphs can be identified from where they cross the x-axis.

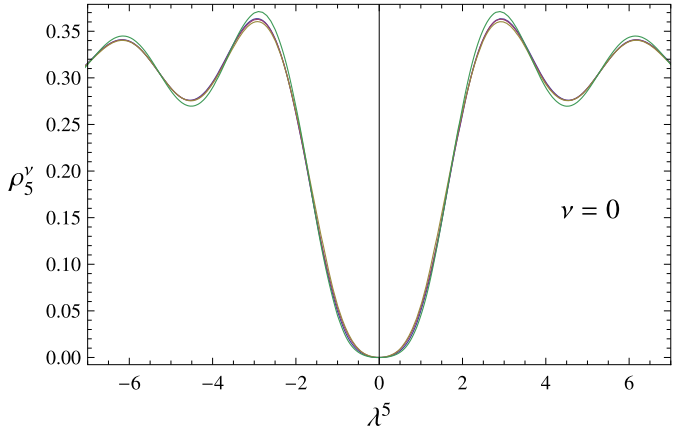

Fig. 8. The spectral density ρ_5^ν for index $\nu = 0$ and $m_f = 1$, compared for different terms in the microscopic effective theory. The small variations come from the graphs with the following values: 1. $a_6^2 = a_7^2 = 0, a_8^2 = 0.04$. 2. $a_6^2 = 0.01, a_7^2 = 0, a_8^2 = 0.04$. 3. $a_6^2 = 0, a_7^2 = 0.01, a_8^2 = 0.04$. 4. $a_6^2 = 0, a_7^2 = 0, a_8^2 = 0.05$.

$$\rho_5^\nu(\lambda^5, m_f) = \left\langle \sum_k \delta\big(\lambda_k^5 - \lambda^5\big)\right\rangle_\nu = \frac{1}{\pi}\,\mathrm{Im}\big[G^\nu\big(-\lambda^5, m_f\big)\big], \qquad (22)$$

where $G^\nu(z, m_f)$ is the resolvent of D_5, obtained as

$$G^\nu(z, m_f) = \left(\frac{\partial}{\partial z}\log Z_{(2|1)}^\nu(m_f, m, m', z, z')\right)\Big|_{z=z',\, m_f=m=m'}. \qquad (23)$$

z and z' are the γ_5-mass which we included in the graded partition function, which comes from the term $z\bar\psi\gamma_5\psi$. z_f is always set to 0. The effect of including the a_6^2 and a_7^2 term, is shown in Figs. 8 and 9.

We see that ρ_5^ν is 0 at the origin as required, since ρ_5^ν is given by the average of $\sum_k \delta(\lambda_k^5 - \lambda^5)\Pi_j(\lambda_j^5)$ which will always be 0 at the origin.

Very recently, two lattice QCD studies [10,11] have demonstrated that the quenched predictions for the microscopic spectra from Wilson chiral perturbation theory, can be matched to the lattice data.

6. Conclusion

We have considered the effect of a non-zero lattice spacing, in the low-energy effective QCD partition function, for one flavor in

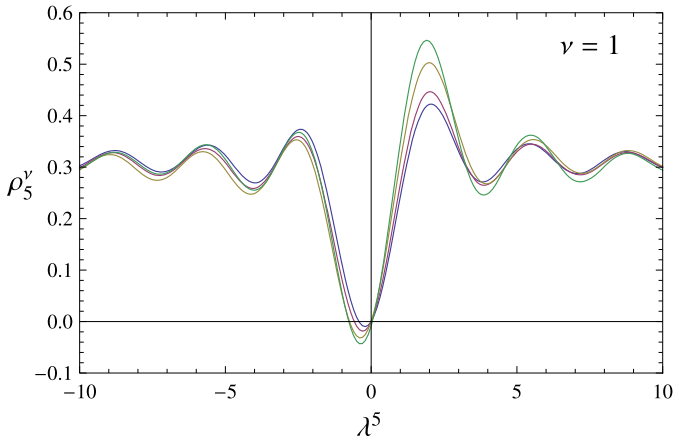

Fig. 9. The spectral density ρ_5^ν for index $\nu = 1$ and $m_f = 1$, compared for different terms in the microscopic effective theory. The highest peak is for $a_6^2 = -0.5, a_8^2 = 1$, the 2nd largest is $a_7^2 = -0.5, a_8^2 = 1$, the 3rd is $a_6^2 = -0.3, a_8^2 = 1$ and the smallest is just $a_8^2 = 1$, where the value is 0 if not mentioned.

the ϵ regime. With this we explored the behavior of the chiral condensate for QCD. We saw that for Z^ν, the zero at the origin for $a_8^2 = 0$, coming from the ν zero eigenvalues, were spread out into ν zeros for $a_8^2 \neq 0$. This was tested for a variety of values for a_8^2. It was observed in all plots, that the number of real zeros was equal to $|\nu|$.

We also explored how the full condensate was build up. This we compared to the continuous case. For $a_8^2 \neq 0$ we observed how the full condensate started to make a damped oscillation, when we summed from $-\nu$ to ν.

We ended with showing the ϵ regime spectral densities of the Wilson Dirac operator, and especially focused on the effect of a_6^2 and a_7^2. We saw how a_6^2 and a_7^2 had a very similar effect of shifting the height of the peaks. We have checked that the densities are zero at the points dictated by QCD. It was also checked that $\int_{-\infty}^{\infty} \rho_\chi^\nu(\lambda^W)\, d\lambda^W = \nu$, which shows that the definition of Z^ν is consistent with the interpretation of ν as the index of D_W.

Acknowledgements

I would like to thank Poul Henrik Damgaard and Kim Splittorff for discussions.

References

[1] H. Leutwyler, A.V. Smilga, Phys. Rev. D 46 (1992) 5607.
[2] G. Akemann, P.H. Damgaard, K. Splittorff, J.J.M. Verbaarschot, Phys. Rev. D 83 (2011) 085014, arXiv:1012.0752 [hep-lat].
[3] J. Gasser, H. Leutwyler, Phys. Lett. B 188 (1987) 477.
[4] S.R. Sharpe, R.L. Singleton, Phys. Rev. D 58 (1998) 074501, hep-lat/9804028.
[5] P.H. Damgaard, K. Splittorff, J.J.M. Verbaarschot, Phys. Rev. Lett. 105 (2010) 162002, arXiv:1001.2937 [hep-th].
[6] P.H. Damgaard, Nucl. Phys. B 556 (1999) 327, hep-th/9903096.
[7] P.H. Damgaard, J.C. Osborn, D. Toublan, J.J.M. Verbaarschot, Nucl. Phys. B 547 (1999) 305, hep-th/9811212.
[8] G. Akemann, P.H. Damgaard, K. Splittorff, J. Verbaarschot, PoS LATTICE2010 (2010) 079, arXiv:1011.5121 [hep-lat].
[9] K. Splittorff, J.J.M. Verbaarschot, arXiv:1105.6229 [hep-lat].
[10] P.H. Damgaard, U.M. Heller, K. Splittorff, arXiv:1110.2851 [hep-lat].
[11] A. Deuzeman, U. Wenger, J. Wuilloud, arXiv:1110.4002 [hep-lat].